Embryonic MGE Precursor Cells Grafted into Adult Rat Striatum Integrate and Ameliorate Motor Symptoms in 6-OHDA-Lesioned Rats

Verónica Martínez-Cerdeño,[1,2,6,*] Stephen C. Noctor,[1,2,7] Ana Espinosa,[3] Jeanelle Ariza,[1,2] Philip Parker,[1,2] Samantha Orasji,[4] Marcel M. Daadi,[5,8] Krystof Bankiewicz,[5] Arturo Alvarez-Buylla,[1,5] and Arnold R. Kriegstein[1,2,*]

[1]Eli and Edythe Broad Center of Regeneration Medicine and Stem Cell Research at UCSF
[2]Department of Neurology
University of California, San Francisco, 513 Parnassus Avenue, San Francisco, CA 94143, USA
[3]Instituto de Neurociencias de Alicante, CSIC and Universidad Miguel Hernández, E-03550 San Juan de Alicante, Spain
[4]Leiden University Medical Center, 2300 Leiden, The Netherlands
[5]Department of Neurosurgery, University of California, San Francisco, 10 Kirkham Street, San Francisco, CA 94143, USA
[6]Present address: Institute for Pediatric Regenerative Medicine, Shriners Hospital of Northern California and Department of Pathology and Laboratory Medicine, UC Davis, 2425 Stockton BLVD, Sacramento, CA 95817, USA
[7]Present address: Department of Psychiatry and Behavioral Sciences, UC Davis M.I.N.D. Institute, 2805 50th Street, Sacramento, CA 95817, USA
[8]Present address: Department of Neurosurgery, Stanford University School of Medicine, 1201 Welch Rd, Stanford, CA 94305, USA
*Correspondence: vmartinezcerdeno@ucdavis.edu (V.M.-C.), kriegsteina@stemcell.ucsf.edu (A.R.K.)
DOI 10.1016/j.stem.2010.01.004

SUMMARY

We investigated a strategy to ameliorate the motor symptoms of rats that received 6-hydroxydopamine (6-OHDA) lesions, a rodent model of Parkinson's disease, through transplantation of embryonic medial ganglionic eminence (MGE) cells into the striatum. During brain development, embryonic MGE cells migrate into the striatum and neocortex where they mature into GABAergic interneurons and play a key role in establishing the balance between excitation and inhibition. Unlike most other embryonic neurons, MGE cells retain the capacity for migration and integration when transplanted into the postnatal and adult brain. We performed MGE cell transplantation into the basal ganglia of control and 6-OHDA-lesioned rats. Transplanted MGE cells survived, differentiated into GABA+ neurons, integrated into host circuitry, and modfied motor behavior in both lesioned and control rats. Our data suggest that MGE cell transplantation into the striatum is a promising approach to investigate the potential benefits of remodeling basal ganglia circuitry in neurodegenerative diseases.

INTRODUCTION

Parkinson's disease (PD) affects approximately 150 per 100,000 people in Europe and the United States of America. PD is characterized by motor impairments as well as cognitive and autonomic dysfunction and disturbances in mood. Motor aspects of PD, including resting tremor, rigidity, and bradykinesia, are the earliest symptoms and have a significant impact on quality of life. Existing treatments can attenuate the symptoms of PD but there is no cure. The motor symptoms of PD result primarily from the loss of dopamine-containing neurons in the substantia nigra pars compacta (SNc) that extend axonal projections to the striatum and release dopamine (for review, see Litvan et al., 2007). The SNc and the striatum belong to the basal ganglia, a network of nuclei, which integrate inhibitory and excitatory signals to control movement. Loss of SNc cells in PD reduces the amount of dopamine release into the striatum, producing a neurotransmitter imbalance that inhibits the output of the basal ganglia and produces hypokinetic signs (for review, see DeLong and Wichmann, 2007) associated with overactivity of the indirect, striatal-pallidal pathway.

The striatum is composed of three classes of neurons. The medium spiny neurons are GABAergic projection neurons that account for 95% of striatal neurons, express calbindin and substance P, give rise to nearly all striatal outputs, and receive nearly all the extrastriatal inputs (Tepper and Bolam, 2004). The large spiny cholinergic neurons that account for 3%–4% of striatal neurons are excitatory and modulate the sub- and suprathreshold responses of the medium spiny neurons to cortical and/or thalamic inputs (Tepper and Bolam, 2004). The small spiny neurons represent the remaining 1%–2% of striatal neurons in the striatum. They are GABAergic interneurons and provide the main source of inhibition for medium spiny neurons (Koós and Tepper, 1999; Koos et al., 2004; Plenz and Kitai, 1998). There are three subtypes of small spiny neurons based on the patterns of marker expression: one subtype that expresses calretinin (CR), a second subtype that expresses parvalbumin (PV), and a third subtype that expresses somatostatin (Som), NADPH-diaphorase, and NOS (Kawaguchi et al., 1995; Tepper and Bolam, 2004). Each GABAergic interneuron produces a strong inhibitory postsynaptic potential in medium spiny neurons that influences the precise timing of action potential firing. Both excitatory and inhibitory striatal interneurons are important sites of action for neuromodulators in the striatum and act in different but complementary ways to modify the activity of the medium spiny projection neurons (Tepper and Bolam, 2004).

Striatal neurons originate from the embryonic primordium of the basal ganglia, the ganglionic eminences. Inhibitory

GABAergic and cholinergic interneurons are believed to derive from the medial ganglionic eminence (MGE) and perhaps the preoptic area (Anderson et al., 1997b; Deacon et al., 1994; Olsson et al., 1995; Zhao et al., 2003). GABAergic interneurons may have mixed origins. The CR[+] subclass of interneurons derives mostly from the MGE, but as many as 10% may be derived from the LGE (Marin et al., 2000). The PV[+] subclass of interneurons derives entirely from the MGE (Marin et al., 2000). Transplantation studies suggest that Som[+] interneurons may originate from both the LGE and MGE (Olsson et al., 1998), although the expression pattern of the transcription factor Nkx2.1, which is required for the specification of MGE derivates, suggests that Som^{+} cells are derived only from the MGE (Marin et al., 2000). The embryonic MGE also produces a substantial number of neocortical interneurons that migrate long distances over a tangential pathway to the dorsal neocortex where they mature into local circuit GABAergic interneurons (Anderson et al., 1997a, 1999; Lavdas et al., 1999; Wichterle et al., 1999). MGE cells retain the capacity for dispersal and integration when transplanted heterochronically into neonatal or adult brain (Grasbon-Frodl et al., 1997; Olsson et al., 1997; Wichterle et al., 1999), develop into mature neurons when retransplanted into the ganglionic eminences (Butt et al., 2005), and can significantly increase the levels of inhibition exerted on neocortical projection neurons when grafted into the neocortex (Alvarez-Dolado et al., 2006).

The most widely used treatment for PD is administration of the dopamine precursor levodopa, which improves motor behavior but can also produce undesirable side effects including dyskinesias. Surgical approaches involve electrical stimulation or ablation of the motor thalamus, the subthalamic nucleus (STN), or the globus pallidus. Additional therapeutic strategies involve transplantation of adult or embryonic dopamine-releasing tissues or stem cells. However, these treatments have drawbacks, and in some cases have produced disabling side effects (Piccini, 2002). We have investigated a novel approach to treating motor symptoms in the 6-hydroxydopamine (6-OHDA) rat model of PD via a nondopamine-based strategy to modify circuit activity in the basal ganglia. We took advantage of the established properties of MGE cells and transplanted them into the striatum of 6-OHDA-treated rats to lower striatal activity. Transplanted MGE cells migrated from the site of injection, dispersed throughout the host striatum, acquired a mature neuronal phenotype, and expressed neuronal and GABAergic markers. In addition, transplanted MGE cells expressed a variety of markers characteristic of striatal GABAergic interneurons, including CB, CR, PV, and Som. Finally, we show that the transplanted MGE cells became physiologically mature, integrated into the host circuitry, and improved the motor symptoms of 6-OHDA-treated rats. Our results indicate that the transplantation of GABAergic interneurons alters striatal circuitry in the rat 6-OHDA model of PD and modifies the motor behavior of both lesioned and control rats.

RESULTS

### MGE Cells Survive up to 1 Year after Transplantation into the Adult Striatum

We dissected MGE cells expressing the GFP reporter protein from embryonic day 14.5 (E14.5) rats, dissociated the cells, and transplanted them into the striatum of 6-OHDA rats. The fate of the cells was determined at various time points after transplantation (approximately 4000 cells obtained from 10 embryos). The MGE cells in suspension were analyzed prior to transplantation via immunohistochemical markers. We found that 75.1% ± 2.0% expressed the immature neuronal marker MAP2, and 32.7% ± 1.4% expressed the mature neuronal marker NeuN. Some cells expressed the inhibitory neurotransmitter GABA (45.5% ± 2.1%) and the GABA synthesis enzyme GAD67 (57.7% ± 2.9%). The dissociated MGE cells also expressed striatal interneuronal markers such as calretinin (CR, 67.0% ± 2.9%), parvalbumin (PV, 51.9% ± 3.6%), somatostatin (Som, 54.1% ± 2.9%), or the striatal projection marker calbindin (CB, 44.8% ± 2%). Some of these markers were colocalized. A small portion of the MGE cells expressed markers of precursor cells such as Nestin (7.4% ± 1.3%), Ki67 (5.9% ± 1.0%), and 4A4 (2.1% ± 0.5%). We concluded that the injected cells were composed primarily of immature or mature neurons (up to 75%) that express striatal interneuronal or projection cell markers and a minority of proliferating cells (up to 7%).

We injected approximately 250,000 cells into the striatum of each animal and found that many of the transplanted cells did not survive longer than 3 weeks after the transplantation. At 4 weeks after transplantation, approximately 1% (2613 ± 156) of the transplanted cells remained. These cells persisted and their number did not decrease further for up to 1 year after transplantation. Our cell survival rate is similar to that reported by other groups who have transplanted embryonic cells into adult rat striatum after 6-OHDA lesions (see Terpstra et al., 2007). To determine whether some of the MGE cells remained proliferative after transplantation, we labeled fixed tissue with Ki67, a marker expressed by dividing cells, and did not find Ki67^{+} MGE cells at any time point after the transplantation (1, 2, and 4 days, 4 weeks, 8 weeks, and 12 weeks), indicating that the MGE cells ceased dividing soon after transplantation.

Transplanted MGE Cells Migrate throughout the Striatum

We examined the morphology of the surviving MGE cells at several time points after transplantation. At 3 and 7 days posttransplantation, GFP^{+} cells had moved away from the site of injection and many had the characteristic morphology of migrating neurons including an oblong soma with a leading process and a trailing process. At 2 weeks posttransplantation, many of the GFP-MGE cells had migrated 2.0 to 2.5 mm in all directions from the site of transplantation and some of the transplanted cells had migrated up to 3.5 mm. At 2 weeks posttransplantation, the cells appeared more mature with an oval soma and abundant neuritic processes. The vast majority of the GFP^{+} cells were found in the striatum, indicating that the MGE cells did not migrate beyond the borders of the adult striatum (Figure 1A). The few cells found in the cortex were probably derived from the injection track. At 4 weeks posttransplantation, the majority of transplanted MGE cells had a mature appearance with an oblong cell body and multiple processes extending at least 50 μm from the soma lesions (see Figure 1B). The transplanted cells had very extensive and ramified processes that could be observed as GFP[+] fibers or puncta throughout the transplanted striatum.
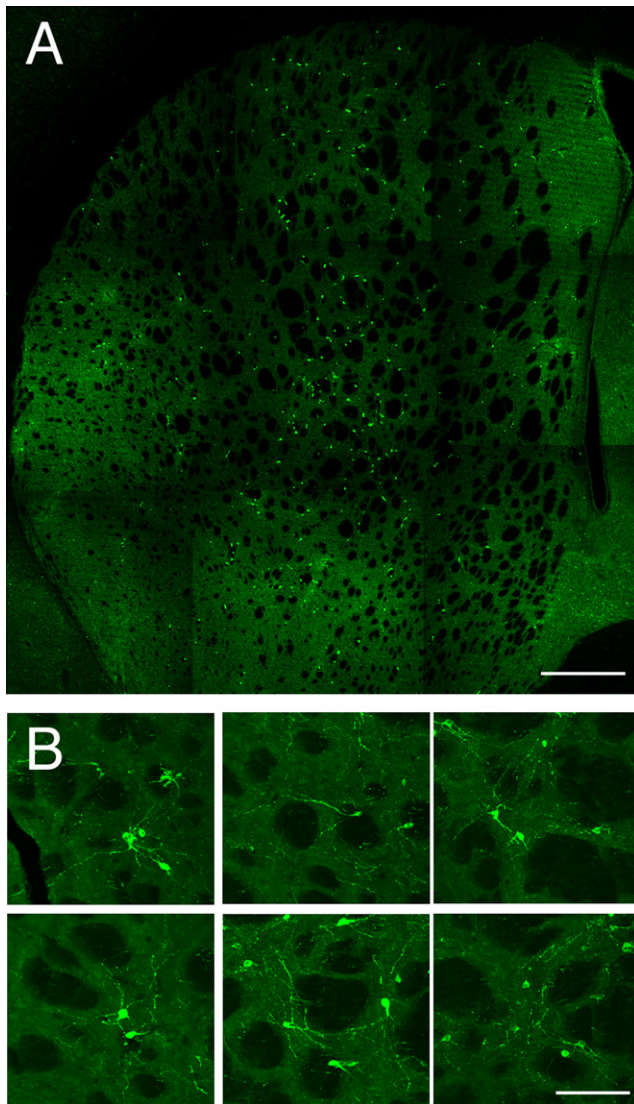
Figure 1. Transplanted MGE Cells Migrated Long Distances from the Site of Injection throughout the Striatum

(A) Striatum 4 weeks after transplantation. The transplanted GFP-MGE cells migrated up to 2.5 mm in all directions from the sites of injection but did not migrate beyond the borders of the striatum.

(B) Eight weeks after transplantation, the MGE cells had a mature appearance. Most MGE cells had an oblong body shape and numerous processes that could be traced up to hundreds of μm from the soma. The GFP$^+$ processes were present throughout the striatum even in areas far away from GFP-MGE cell bodies. Scale bars represent 0.5 mm in (A) and 25 μm in (B).

GFP$^+$ processes occupied the entire striatum, including areas remote from the injection sites (Figure 1B). GFP$^+$ neuritic processes studied at higher magnification did not have spines, suggesting that they were not medium spiny projection neurons.

Most Transplanted MGE Cells Develop into Inhibitory GABA$^+$ Cells

We examined the fate of the transplanted MGE cells by quantifying the percentage that expressed cell-specific markers at 4,

8, and 12 weeks after transplantation. 4 weeks posttransplantation, the majority of the MGE cells expressed the mature neuronal marker NeuN (75% ± 6%, n = 676 cells). We also found that most of the transplanted cells expressed markers of GABAergic neurons, including GABA (75% ± 4%, n = 294 cells), the GABA-synthesizing enzyme GAD (60% ± 11%, n = 382 cells), and the GABA transporter GAT1 (50% ± 9%, n = 380 cells), indicating that the majority of MGE cells became GABAergic neurons (Figure 2). Some of the MGE cells expressed markers of striatal interneuron subtypes such as CR (8.3% ± 0.5%, n = 473 cells), PV (0.5% ± 0.5%, n = 320 cells), Som (1% ± 0.5%, n = 300 cells), or nitric oxide synthase (NOS, 1% ± 0.7%, n = 337 cells). None of the transplanted MGE cells (n = 459 cells) expressed the cholinergic interneuron marker ChAT, which is expressed by striatal excitatory interneurons. Some MGE cells expressed markers typical of striatal projection neurons such as CB (24% ± 7%, n = 300 cells), but only at 4 weeks after transplantation. The expression of CB by transplanted MGE cells was transient, decreasing significantly by 8 weeks after transplantation. Some transplanted MGE cells expressed substance P (6% ± 2%, n = 193 cells; Figure 2) but were negative for markers related to dopamine synthesis such as tyrosine hydroxylase (TH), vesicular monoamine transporter 2 (VMAT), dopamine transporter (DAT), or the marker of adult medium spiny projection neurons, DARPP 32. However, half of the transplanted MGE cells (49.43% ± 6%, n = 172 cells) expressed the transcription factor NKX2.1, which is required for the specification of PV$^+$ and SOM$^+$ striatal interneurons. Together, these data indicate that most MGE cells transplanted into adult striatum differentiated into local GABAergic interneurons within 4 weeks and expressed a range of cell-specific markers that are normally expressed in the adult rat striatum.

We tested whether the pattern of marker expression of transplanted cells changed at later time points after transplantation. We found that marker expression was preserved at 8 and 12 weeks with some notable exceptions. The percentage of MGE cells that expressed Som rose from 1% to 10% ± 3% (n = 343 cells) by 12 weeks after transplantation. In addition, we found that the percentage of MGE cells expressing the calcium binding proteins was greatly reduced (CR, 2% ± 1%, n = 258 cells; CB, 2% ± 1.5%, n = 270 cells; PV, 0%, n = 136 cells). Interestingly, we noted that close to the injection site, transplantation of the MGE cells induced transient expression of CR and CB by host striatal cells. At 4 weeks after transplantation, we noted strong CR and CB expression in host cells, but this pattern of expression was not present 8 weeks after transplantation. Host cells in control animals that received an injection of vehicle only did not express CR or CB, indicating that the expression of CR and CB in host cells was probabaly due to presence of the transplanted MGE cells. Thus, the expression of CB by the MGE transplant cells that we noted at 4 weeks was not a strong indication that the MGE cells had differentiated into striatal projection neurons because both host and transplant cells expressed CB transiently at 4 weeks, and because the vast majority of MGE cells did not express CB at 8 weeks after transplantation and at subsequent time points studied.

One fourth of the transplanted MGE cells (25% ± 4%) were NeuN negative. The NeuN-negative cells stained positive for the myelin protein, CNPase, suggesting that a subpopulation
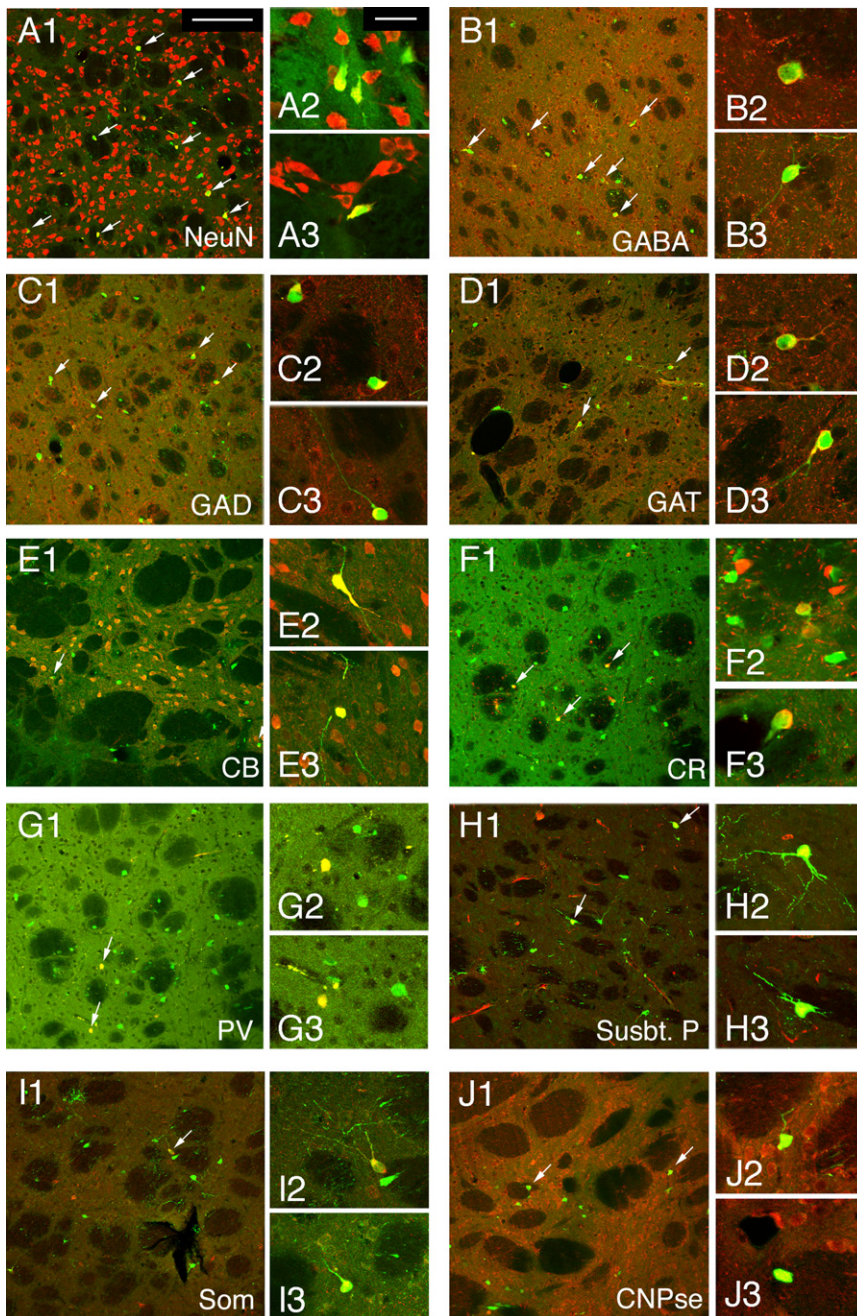
Figure 2. Most MGE Cells Adopted an Inter-neuronal Fate when Transplanted into the Adult Striatum

(A) Four weeks after transplantation, most MGE cells expressed the mature neuronal markers NeuN (75% ± 6%).

(B–D) Most MGE cells also expressed markers related to GABA storage or synthesis such as GABA (B, 75% ± 4%), GAD (C, 60% ± 11%), and GAT (D, 50% ± 9%).

(E–I) Some transplanted MGE cells also expressed interneuron subtype markers CB (E, 24% ± 7%), CR (F, 8.3% ± 0.5%), PV (G, 0.5% ± 0.5%), Substance P (H, 6% ± 2%), and Somatostatin (I, 1% ± 0.5%).

(J) One quarter of the MGE cells transplanted into the striatum (25% ± 4%) expressed the oligodendrocyte marker CNPase. Arrows point to examples of MGE cells that stained positive for each marker, and insets for each panel (labeled 2 and 3) show higher power examples of immunopositive cells.

Scale bar represents 30 μm in (A1) and applies to lower-power images shown in (A1)–(J1); scale bar represents 10 μm in (A2) and applies to all higher-power inset images (A2–J2 and A3–J3).

were relatively small, the size of CR$^+$ and PV$^+$ transplanted MGE cells was similar to that of striatal host cells (CR$^+$ cells = 23.5 ± 1.4 × 19.5 ± 1.5 μm, PV$^+$ cells = 25.9 ± 0.9 × 20.2 ± 0.7 μm, CB$^+$ cells = 30.4 ± 0.6 × 23.6 ± 0.5 μm) and similar to cell size previously reported for striatal neurons in vivo (Kawaguchi et al., 1995; Tepper and Bolam, 2004). Thus, our data suggest that transplanted MGE cells differentiated into cell types similar to those of the host striatum.
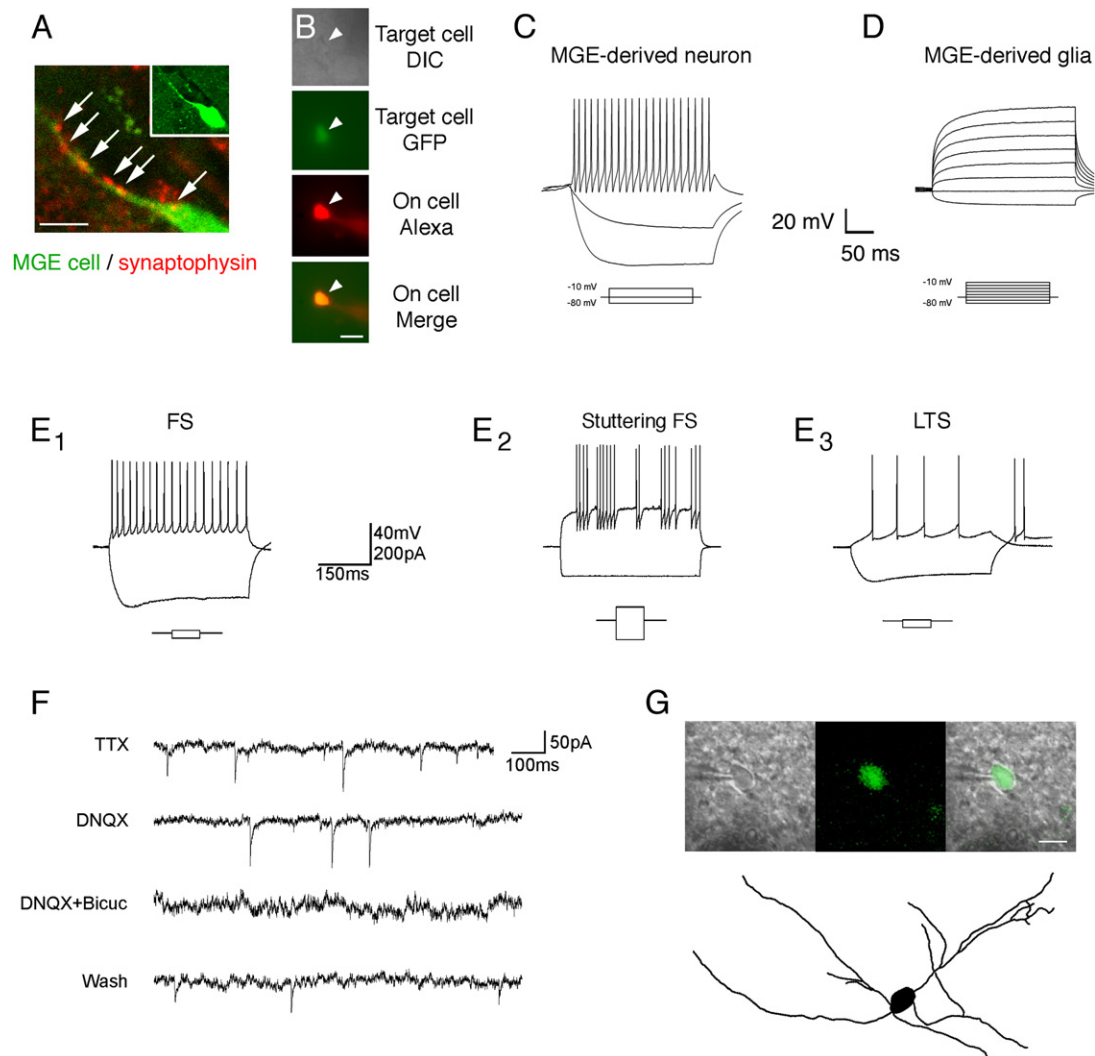
Transplanted MGE Cells Integrate into the Striatal Circuitry

We next examined whether the transplanted MGE cells established synaptic connections and became functionally integrated into the host striatum. We found that 4 weeks after transplantation, 67% ± 3% of the GFP$^+$ MGE cells

of MGE cells differentiated into oligodendrocytes. None of the MGE cells that were transplanted into the striatum expressed GFAP, indicating that transplanted cells did not differentiate into astrocytes. The 3:1 ratio of neuronal to glial cells that we observed at 4 weeks was maintained at 8 and 12 weeks post-transplantation.

We also analyzed the cell soma size of transplanted MGE cells that stained positive for cell-specific markers at 4 weeks after transplantation (n = 660 cells obtained from 7 embryos): GFP-CR$^+$ cells were 25.6 ± 0.6 × 21.0 ± 0.5 μm, GFP-PV$^+$ cells were 26.6 ± 0.8 × 21.3 ± 0.6 μm, and GFP-CB$^+$ were 21.3 ± 0.65 × 17.45 ± 0.5 μm. With the exception of CB$^+$ cells that

(n = 193 cells) expressed synaptophysin puncta along their processes, indicating the presence of synapses (Figure 3A). Electrophysiological recordings provided further evidence that the MGE cells became functionally integrated into the host striatum. We obtained whole-cell patch-clamp recordings from the GFP$^+$ MGE cells at 5 to 20 weeks after transplantation to examine their basic membrane properties (n = 44 cells). We included Alexa-594 dye in the patch electrodes to confirm that recordings were obtained from targeted GFP-expressing transplant cells or Texas Red dextran for morphological analysis of the recorded cells (Figure 3B). Most of the transplanted MGE cells displayed the physiological properties of neurons (37/44 cells): fast sodium

Figure 3. MGE Cells Transplanted into the Striatum Displayed the Basic Membrane Properties Characteristic of Mature Forebrain Interneurons and Showed Evidence of Synaptic Integration

(A) 67% of the MGE cells (green) expressed the synapse marker synaptophysin (red) along their processes (white arrows).

(B) We obtained whole-cell patch-clamp recordings from transplanted cells up to 20 weeks after transplantation. Alexa-594 (red) was included in the fill solution of the glass microelectrode to confirm that recordings were obtained from targeted GFP-expressing MGE transplant cells.

(C) Most MGE cells (37/44) fired repetitive nonaccommodating action potentials with large afterhyperpolarizations as is common for MGE-derived interneurons.

(D) A small percent of the transplanted MGE cells that were recorded from (n = 7/44) did not exhibit neuronal membrane properties and did not fire action potentials when stimulated with a series of depolarizing currents, consistent with glial cell identity.

(E_1) Most MGE neurons were fast spiking (FS) cells and did not fire rebound action potentials after hyperpolarization.

(E_2) The FS population included stuttering FS cell subtypes.

(E_3) The second most common cell type was low-threshold-spiking (LTS) cells. These cells displayed much lower spiking frequencies than did FS cells and displayed two or more rebound spikes in response to hyperpolarization.

(F) Transplanted cells demonstrated both AMPA and GABA-mediated spontaneous synaptic events.

(G) A transplanted MGE cell filled with Texas red-dextran demonstrated the branched aspiny processes that are characteristic of striatal interneurons.

Scale bars represent 3 μm in (A), 5 μm in (B), and 10 μm in (G).

action potentials blocked by TTX, relatively high input resistances (324.6 ± 47.1 MΩ), and frequent spontaneous synaptic activity (Figure 3C). The remaining 7/44 cells had properties that were consistent with a glial phenotype: no fast currents, very low input resistances (115.0 ± 13.4 MΩ), and no spontaneous synaptic inputs (Figure 3D). These data are consistent with our immunohistochemical results.

All recorded neurons (n = 37) displayed passive and active properties consistent with forebrain GABAergic interneurons, and the percentage breakdown of cells within interneuron subtypes was consistent with our immunohistochemistry results. The majority of transplanted MGE cells (50.0%) was fast-spiking (FS) with low input resistances, fast time constants, and hyperpolarized resting membrane potentials. These cells showed

extremely high-frequency firing with little adaptation and large afterhyperpolarizations and did not fire rebound action potentials after hyperpolarization (Figure 3E₁). Within the FS cell population were examples of both delayed FS and stuttering FS cells (see Figure 3E₂). The second most common cell type we recorded were low-threshold-spiking cells (38.5%), also known as burst-spiking nonpyramidal cells, which had higher input resistances, slower time constants, and more depolarized resting membrane potentials. These cells displayed much lower spiking frequencies than FS cells and displayed two or more rebound spikes in response to hyperpolarization (Figure 3E₃). Finally, rebound-regular-spiking nonpyramidal (R-RSNP) cells were also encountered (7.7%). These cells had high input resistances, long time constants, and hyperpolarized resting membrane potentials. R-RSNP cells fired a single rebound spike in response to hyperpolarization. We did not encounter nonrebounding RSNP cells while recording from the transplanted MGE cells. One cell, which was omitted from classification, had fast-spiking properties but a relatively high input resistance, exceptionally strong hyperpolarization-activated cation current, and extensive rebound spiking in response to hyperpolarization. To segregate AMPAergic and GABAergic miniature synaptic currents, TTX was bath-applied to isolate miniature synaptic events while DNQX (to block AMPA events) and bicuculline (to block GABA_A receptor-mediated events) were locally applied. The cells showed typical rates (1.9 ± 0.45 events/s) and amplitudes (57.45 ± 0.95 pA) of miniature synaptic events and received both glutamatergic and GABAergic inputs at a relative frequency of about 1.5:1. Simultaneous application of DNQX and bicuculline eliminated all miniature synaptic events (Figure 3F). Some of the cells were filled with Texas Red-dextran for morphological analysis of recorded cells. Transplanted MGE cells possessed numerous ramified processes that extended hundreds of μm away from the cell body (Figure 3G). These data suggest that the transplanted cells receive functional synaptic inputs from local striatal inhibitory cells as well as from excitatory cortical and/or thalamic cells, which provide the main glutamatergic input to the striatum. The membrane properties of the transplanted cells were consistent with the membrane properties recorded from host striatal interneurons (Kawaguchi, 1993), and similar to those observed in MGE-derived interneurons transplanted into the cerebral cortex (Alvarez-Dolado et al., 2006; Butt et al., 2005). Together, these data support the conclusion that the majority of the transplanted MGE cells become inhibitory interneurons that are synaptically integrated into the host striatal circuitry.

MGE Cell Striatal Transplants Ameliorate the Behavioral Symptoms of 6-OHDA-Lesioned Rats

To test the effect of transplanted MGE cells on the behavior of 6-OHDA-lesioned rats, we performed a series of behavioral tests on each rat before and after transplantation or treatment (Figure S1A available online) and analyzed the data via a 1-way ANOVA model across time. We used week 5 as the baseline time point and expressed the results for each of the subsequent behavioral tests relative to the week 5 results. We performed a series of multiple observations among groups: the 6-OHDA + MGE cell group, the 6-OHDA and no transplant group, the 6-OHDA + sham surgery group, and finally the 6-OHDA + dead MGE cell group. The graphs display the change in behavior from the baseline for each group.
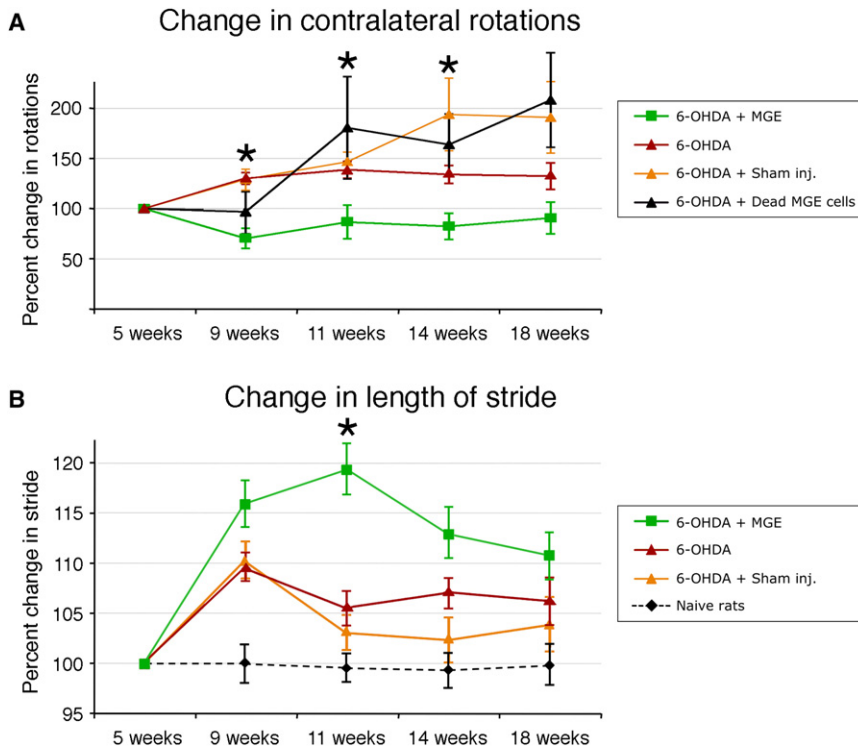
Rotation under Apomorphine

Upon administration of apomorphine, rats with a unilateral 6-OHDA lesion rotate more to the contralateral side (with respect to the lesioned side) than to the ipsilateral side. Control rats rotate equally in both directions. For our studies, we followed the convention of Ungerstedt and colleagues (Ungerstedt, 1971) and considered the 6-OHDA-treated rats as hemi-Parkinsonian when rotations to the contralateral side were at least four times greater than rotations to the ipsilateral side. We compared the number of contralateral rotations for the experimental and control groups and found that the number of rotations decreased in the MGE-treated group (n = 18 rats) after transplantation, but increased in the control groups (n = 12 rats; Figure 4A). ANOVA showed that the difference between groups was statistically significant at weeks 9, 11, and 14 (p < 0.01). Furthermore, postcomparison tests showed that the MGE cell-treated group rotated significantly less than the 6-OHDA and sham-injected control (n = 11 rats) groups at 9, 11, and 14 weeks posttransplantation, and significantly less than the dead MGE cell-injected control group (n = 6 rats) at 11, 14, and 18 weeks. These results indicate that transplantation of live MGE cells into the striatum decreased apomorphine-induced rotations in 6-OHDA-lesioned rats (Figure 4A).

Stride Length

We next compared the length of stride between experimental and control groups to test the effects of MGE cell transplantation on additional motor behaviors. The rats' feet were dipped in black ink and they were placed in a 1 m long runway that was covered with paper to capture the rats' footsteps (see Figures S1D–S1F). We found that the length of stride of the 6-OHDA-treated rats increased after MGE cell transplantation (n = 21 rats) and was significantly longer than that of the 6-OHDA-treated (n = 12 rats), sham-injected (n = 11 rats), and dead MGE cell-injected (n = 6 rats) control groups at week 11 (p = 0.02, Figure 4B).

MGE Cell Striatal Transplants Alter the Motor Performance of Wild-Type Rats

The above results indicate that MGE cells transplanted into 6-OHDA-treated rats can modify their behavior. We next tested whether MGE transplantation into the striatum of naive unlesioned animals had any effect. We transplanted MGE cells into intact rats and examined their behavior via the assays described above. The rotation under apomorphine test was not significantly different in the naive rats injected with MGE cells (n = 6 rats) compared to nontransplanted controls (n = 6 rats). In contrast, the stride length of the naive rats that received MGE transplants was significantly longer than that of control untreated rats (p < 0.001, see Figure 5A). We also performed an open field activity test in naive unlesioned control, 6-OHDA-injected, and MGE-transplanted naive unlesioned rats. We tested the level of motor activity in an open field during a 5 min period and found that MGE cells transplanted into naive rats (no 6-OHDA treatment) produced a level of activity (UM) that was significantly higher (1101 ± 39 UM) than that in naive rats without any treatment (912 ± 104 UM). We also found that 6-OHDA-injected rats had lower motor activity levels than naive rats (453 ± 69 UM). The increase of motor activity in naive rats that received MGE cell

Figure 4. MGE Cell Transplantation Ameliorates the Behavioral Deficits of 6-OHDA Lesions

(A) Rotation test. 6-OHDA-lesioned rats that received MGE cell transplantation (n = 18) performed fewer contralateral rotations under apomorphine stimulation than nontransplanted 6-OHDA controls (n = 15), 6-OHDA-lesioned rats that received sham injection (n = 11), or dead MGE cells (n = 10). ANOVA showed that the difference between groups was significant at 9, 11, and 14 weeks (asterisks). Postcomparison analysis showed that the MGE group rotated significantly less than the 6-OHDA-treated control groups at 9, 11, and 14 weeks. Error bars depict standard error of the mean.

(B) Length of stride test. 6-OHDA-lesioned rats that received MGE cell transplantation (n = 18) had a longer stride than did nontransplanted 6-OHDA controls (n = 15) and 6-OHDA-lesioned rats that received sham injection (n = 11). Naive rats (n = 10) are included for comparison. ANOVA showed that the difference between groups was significant at 11 weeks. Postcomparison analysis showed that the MGE group had a significantly longer stride than the 6-OHDA-lesioned control groups at 11 weeks (asterisk). See also Figure S1.

transplants versus naive rats is reflected in the open field zone map (Figures 5B and 5C).
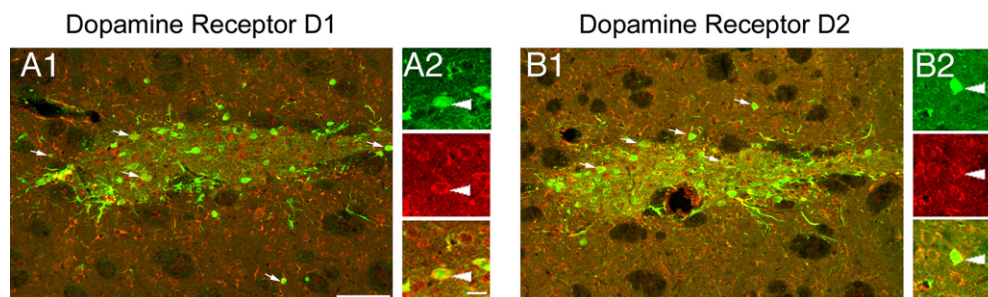
MGE Cells Express D1 and D2 Dopamine Receptors

Apomorphine binds to dopamine receptors expressed by host striatal neurons, which causes rotation in the 6-OHDA rat (Ungerstedt and Arbuthnott, 1970). We found that apomorphine-induced rotational behavior was significantly reduced after MGE transplantation. We asked whether the transplanted MGE cells participated directly or indirectly in this response by examining the expression of dopamine receptors by the transplanted MGE cells. We performed fluorescence immunostaining for dopamine receptor 1 (DR1) and 2 (DR2) and detected the presence of both receptors in the surface of cell soma and

processes of MGE cells 12 weeks after transplantation (Figure 6). These data suggest that apomorphine, and thus dopamine itself, can directly stimulate MGE inhibitory interneurons, potentially modifying rotational behavior and altering the balance of excitation/inhibition in the striatum.

MGE Cells Transplanted in the Subthalamic Nucleus Do Not Migrate, but Survive and Differentiate into Glial Cells

It has been suggested that increasing inhibition in the STN could have beneficial effects in Parkinson's disease (Benabid et al., 2000; During et al., 2001). We therefore investigated whether MGE cells transplanted in the STN survive and differentiate in 6-OHDA-lesioned rats. We characterized the MGE cells 4 weeks

Figure 5. MGE Transplanted Cells Expressed Dopamine Receptors

(A1 and B1) MGE cells (green) expressed the dopamine receptor D1 (red) and dopamine receptor D2 (red).

(A2 and B2) Higher-magnification images showing that the MGE transplant cell (green, white arrowhead) expresses D1 and D2 (red) on the somatic membrane and processes. Merge panel shows colocalization.

Scale bars represent 30 μm for (A1) and (B1) and 3 μm for (A2) and (B2).
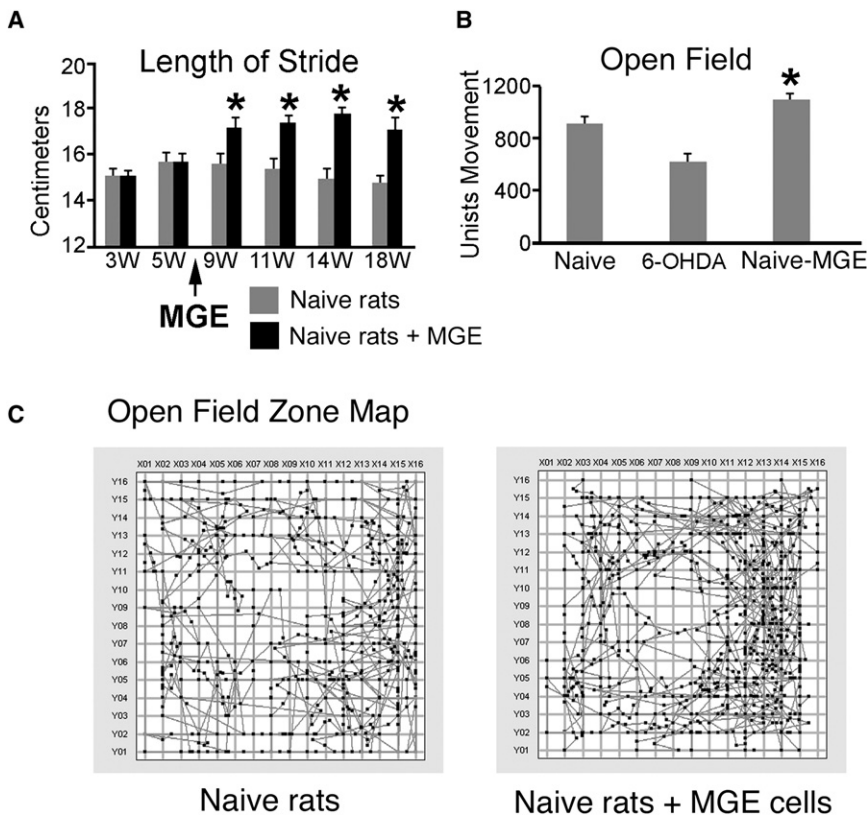
Figure 6. Transplantation of MGE Cells into Control Rats that Had Not Been Lesioned with 6-OHDA Increased the Length of Stride and the Level of Activity

(A) The length of stride was significantly higher in control rats injected with MGE cells (n = 6) than in control rats (n = 16).

(B) Open field tests showed an increase in activity for control animals that received MGE cell transplantation in comparison to control rats.

Error bars depict standard error of the means.

(C) Representative open field zone maps from two rats showing that transplantation of MGE cells into control rats increased the level of motor activity over that of control rats.
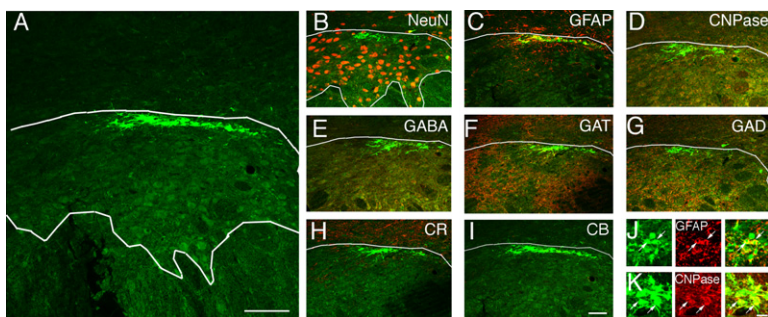
expressed GFAP. Roughly one-third of the MGE cells in the STN also expressed the oligodendrocyte marker CNPase (30% ± 9%, n = 132 cells; Figures 7C, 7D, 7J, and 7K). We found that a small percentage of MGE cells in the STN expressed the GABA transporter GAT1 (13% ± 5%, n = 94 cells; Figure 7F). GAT-expressing cells are most likely astrocytes or oligodendrocytes, which have been shown to express the GAT1 transporter (Pow et al., 2005). These data indicate that unlike the striatum where transplanted MGE cells differentiate into neurons and integrate, most surviving MGE cells transplanted into the STN become glial cells.

after transplantation in the STN. We found that MGE cells transplanted into the STN did not migrate from the site of injection (n = 231 cells, analyzed in 6 rats; Figure 7A). This is in contrast to MGE cells transplanted into striatum, which migrated substantial distances from the site of injection. Moreover, MGE cells in the STN did not differentiate into neurons; none of the 231 transplanted GFP-labeled MGE cells in the STN expressed the neuronal marker NeuN. In contrast, a small number of MGE cells located outside the boundary of the STN did express NeuN (Figure 7B). None of the transplanted MGE cells in the STN expressed the calcium-sequestering proteins CR or CB, or the inhibitory interneuron markers GAD or GABA (Figures 7E and 7G–7I). The majority of MGE cells transplanted into the STN expressed the astrocyte marker GFAP (75% ± 5%, n = 151 cells). In contrast, none of the MGE cells transplanted in the striatum

DISCUSSION

In this study we asked whether MGE cell transplantation could be used to add inhibitory GABAergic interneurons to the striatum and whether this approach might have a beneficial impact on the motor behavior of 6-OHDA hemi-Parkinsonian rats. We transplanted MGE cells from E14.5 rats into the striatum of adult rats. We found that a small population of these cells survived at least 1 year after transplantation, migrated throughout the striatum, differentiated into GABAergic neurons, and became synaptically integrated into the striatal circuitry. We found that

Figure 7. MGA Cells Transplanted in the Subthalamic Nucleus

(A) MGE cells transplanted into the subthalamic nucleus (STN) survived but did not migrate from the site of injection and did not mature into neurons.

(B–K) None of the MGE cells that were transplanted into the STN expressed the neuronal marker NeuN (B), the inhibitory interneuron marker GABA (E) or GAD (G), or the calcium sequestering proteins CR (H) or CB (I). Most MGE cells transplanted into the STN expressed the astrocyte marker GFAP (75% ± 5%, C and J) or the oligodendrocyte marker CNPase (30% ± 9%, D and K). A small percentage of MGE cells in the STN expressed the GABA transporter GAT1 (13% ± 5%, F).

Scale bars represent 25 μm in (A); 25 μm for (I) and (B)–(H); and 5 μm for (K) and (J).

transplantation of MGE cells into the striatum of 6-OHDA-lesioned rats improved motor scores on the apomorphine-stimulated rotation test in this animal model of PD. We also noted that MGE cell transplantation in the striatum increased the motor activity of naive untreated control rats. The ability of MGE cells to differentiate into interneurons appears to depend on the host environment because MGE cells transplanted into the STN differentiated into astrocytes and oligodendrocytes but not neurons. Our data suggest that transplanting MGE cells into striatum is a promising approach for modifying striatal-dependent behaviors. These effects could be clinically relevant in neurodegenerative conditions such as Parkinson's disease.

Transplanted MGE Cells Differentiate into Inhibitory Interneurons that Functionally Integrate into the Striatum

We found that MGE cells transplanted into the striatum survive at least 1 year, migrate from the site of injection, and are widely distributed throughout the striatum. Previous studies have also explored the potential of MGE cell transplantation in the striatum. For example, Campbell et al. (1995) injected MGE cells into the lateral ventricle of embryonic mice and found that while some of the transplanted cells survived, they did not migrate into the striatum. Olsson et al. (1997) transplanted mouse E13.5–E14 MGE cells into the striatum of postnatal day 1, 7, and 21 rats and reported that the cells distributed widely throughout the striatum. Wichterle et al. (1999) transplanted mouse neuronal precursor cells from the MGE, LGE, and cortical ventricular zone into the adult striatum and found that only MGE cells possessed a unique capacity to migrate and differentiate into neurons. Alvarez-Dolado et al. (2006) showed that MGE cells transplanted into postnatal day 3 and 4 striatum differentiated into GABA$^+$ neurons. We confirmed these findings and further demonstrate that MGE cells transplanted into the adult striatum acquire a mature morphological phenotype and differentiate into GABAergic neurons that express markers common to striatal interneurons. Although a small percentage of the transplanted MGE cells survived, their impact on behavior depends on a number of factors including the number of surviving MGE interneurons relative to the normal number of host striatal interneurons. Stereological-based studies estimate that there are approximately 49,000 striatal interneurons in the adult rat: 13,000 CR$^+$ interneurons (Rymar et al., 2004), 15,000 PV$^+$ interneurons (Larsson et al., 2001; Luk and Sadikot, 2001), and 21,000 SOM$^+$ interneurons (West et al., 1996). Therefore, the average number of transplanted MGE cells that survived in our experiments (2613 ± 156 cells, n = 3 rats) could represent up to 5% of the total number of host striatal interneurons. Along with surviving cell numbers, integration of transplanted cells into host tissue is another factor that determines their impact on host behavior. We find that the transplanted MGE cells extend numerous processes throughout the striatum, and our electrophysiological recordings demonstrate that surviving MGE cells integrate within the striatal circuitry. Finally, our behavioral tests show that transplanted MGE cells result in changes in motor behavior in both 6-OHDA-treated and untreated animals. Future studies should explore whether the transplantation of more MGE cells would yield a greater number of surviving interneurons in the host striatum and whether this would have a positive impact

on motor behavior in animal models of PD. In addition, future studies should test the transplantation of multiple cell types to examine for synergistic benefits that could impact different facets of PD.

The embryonic MGE produces striatal and neocortical interneurons that share the expression of several markers (Defelipe et al., 1999; Kawaguchi, 1997; Kubota et al., 1994). Thus, it is likely that the transplanted MGE cells included cells destined to populate both the striatum and the neocortex and that the MGE cells that survived in the striatal transplants are those that had molecular expression characteristics of striatal interneurons. However, we cannot exclude the possibility that the host environment in the striatum also influenced MGE cell fate and marker expression after transplantation. We noted that none of the MGE cells that survived after transplantation in the adult STN express neuronal markers, but many express the astrocyte marker GFAP, which was not expressed by MGE cells after transplantation in the striatum. These data highlight the importance of local environmental cues for the survival and/or fate determination of transplanted MGE cells.

We did not detect GFP$^+$ processes outside of the striatum in the transplanted animals, indicating that the transplanted MGE cells did not differentiate into GABAergic projection neurons. This suggests that the MGE cells integrated within the circuitry of the striatum and that the behavioral changes we observed in transplanted rats may have been due to modification of activity of synapses and/or neurons within the striatum. This could have impacted the activity level of host GABAergic interneurons and/or projection neurons. Future studies will be needed to further understand the physiological integration of MGE cells after transplantation into the adult striatum.

Transplanted MGE Cells Alter Motor Behavior in 6-OHDA-Lesioned and Control Rats

We observed behavioral changes in 6-OHDA-lesioned rats that received MGE cell transplantation, including improved motor scores in the apomorphine rotational test and a temporary increase in the length of stride. These behavioral changes suggest a general improvement of the motor symptoms in 6-OHDA-treated rats after MGE transplantation. A recent study has shown that depriving the striatum of dopaminergic inputs from the substantia nigra creates an imbalance in local circuits that involve GABAergic striatal neurons (Mallet et al., 2006). Previous attempts have been made to modulate basal ganglia activity by enhancing GABA stimulation in animal models of Parkinson's disease. For example, GABA-rich striatal tissue has been transplanted in the substantia nigra of 6-OHDA rats and the tissue survived and induced functional recovery (Winkler et al., 1999). During et al. introduced the gene for the GABA-synthesizing enzyme GAD 65 into the STN of humans through a recombinant adeno-associated viral vector and observed a slower degeneration of dopaminergic neurons (During et al., 2001; Kaplitt et al., 2007). Additionally, gene therapy studies in a rat model of Parkinson's disease that introduced GAD 65 into the STN reported a strong neuroprotective effect on nigral dopaminergic neurons and rescue of the Parkinsonian behavioral phenotype (Lee et al., 2005; Luo et al., 2002). It has recently been shown that striatal interneurons play key roles in basal ganglia function and related disorders by modulating the activity

of striatal projection neurons (Salin et al., 2009). In the experimental stroke animal model, transplanted MGE cells migrated toward lesioned areas of the striatum, integrated into the local circuitry, and rescued motor deficits (Daadi et al., 2009). In the present study, we transplanted MGE cells 6 weeks after the 6-OHDA-induced lesion. We found that the MGE cells differentiated into GABA[+] interneurons within 4 weeks after transplantation and notably improved motor behavior in the 6-OHDA rat model of PD. These results suggest that, in addition to the protective effect described previously, GABAergic cells may be able to improve PD symptoms once the disease is established. Furthermore, the increase in motor behavior that we observed after transplantation of embryonic MGE cells into the striatum of naive control rats indicates that MGE cells may be capable of modifying the intrinsic balance of excitatory and inhibitory signals in the striatum, and thus represent a novel strategy for altering output of the striatum in disease conditions.

The ability of MGE cells to disperse in the striatum, mature, and become functionally integrated into basal ganglia circuitry is probably responsible for the behavioral modifications we observed both in the 6-OHDA-treated and control animals. Our findings are consistent with the interpretation that the transplanted MGE cells release GABA, and this alters the balance of striatal activity to produce behavioral modifications. If this hypothesis is correct, transplanted GABAergic cells would presumably hyperpolarize host striatal neurons and reduce their rate of firing, decrease their inhibitory influence on target cells, and as a result increase the net excitatory output of the basal ganglia. However, other mechanisms could potentially explain the changes in motor behavior we observed after MGE cell transplantation. Our results are similar to those showing that L-dopa administration increases open field activity levels in control rats (Dahl and Götestam, 1989; Ljungberg and Ungerstedt, 1976). Thus, it is also possible that the transplantation of MGE cells induced secondary changes in the striatum that produced or contributed to the behavioral changes (Goto et al., 1997). This possibility is supported by our observation that there was a temporary increase in CB expression by host striatal cells at the site of MGE cell transplantation. It is also possible that the presence of exogenous MGE cells in the adult striatum could have trophic effects and stimulate process outgrowth of host striatal neurons or remaining host dopaminergic processes in the striatum, which could then increase motor activity, although staining for TH did not show an obvious increase. Another possibility is that nonneuronal MGE cells may also have a functional effect. Specifically, the 25% of transplanted MGE cells that matured into oligodendrocytes could release trophic factors such as GDNF, which is known to stimulate regeneration and sprouting of SN neurons (Du and Dreyfus, 2002; Wilkins et al., 2003). Further studies will be required to elucidate the mechanism(s) that produced the altered motor behaviors we observed in the 6-OHDA-treated rats and to explore the full range of cellular effects in the MGE transplant model. Future experimentation in animal models may help determine if there are optimal transplantation sites within the striatum, and experiments to derive MGE-like cells from embryonic stem cells may help overcome potential obstacles such as obtaining a sufficient supply of embryonic MGE cells. MGE cell transplants survive for more than 1 year in the rat and exhibit widespread integration in the adult striatum with functional consequences. Future studies should further explore the clinical potential of these embryonic cells.

EXPERIMENTAL PROCEDURES

Experimental Design

We performed the 6-OHDA lesions on experimental day 1 and behavioral tests at weeks 3 and 5 to select Parkinsonian rats. MGE cells were transplanted at week 6, and behavioral tests were repeated at weeks 9, 11, 14, and 18 (Figure S1A). All animals were treated in accordance with protocols approved by the Institutional Animal Care and Use Committee at UCSF.

6-OHDA Model

We performed a unilateral lesion of the nigrostriatal projection in rats, by using 6-OHDA, which leads to the loss of dopaminergic cells in the SNc through retrograde transport and loss of dopaminergic terminals in the striatum through axonal disruption (Berger et al., 1991). We perfused a subset of animals (n = 5) 4 weeks after lesion and immunostained the SNc for tyrosine hydroxylase (TH), a rate-limiting enzyme in the synthesis of dopamine, to label dopaminergic cells. The SNc ipsilateral to the 6-OHDA injection did not have TH^{+} cells or processes, whereas the contralateral side retained the normal TH[+] cell components (Figure S1B). To evaluate the 6-OHDA surgeries in vivo, we performed behavioral testing as described below.

6-OHDA Surgery

Adult female rats (n = 75) were anesthetized with ketamine (90 mg/kg) and xylazine (7 mg/kg) and immobilized within a stereotaxic frame in flat skull position. The coordinates for the nigrostriatal bundle were determined based on the Paxinos and Watson adult rat brain atlas (Paxinos and Watson, 1982). A midsagittal skin incision was made on the scalp, a hole was drilled through the skull, and a glass capillary micropipette with a 50 μm diameter tip was located within the nigro-striatal pathway. The micropipette was filled with a solution of 6-OHDA (Sigma, MO): 0.5 ml of 6-OHDA (4 mg/ml) plus 0.02% ascorbic acid in saline. The 6-OHDA solution was slowly injected and the micropipette was kept at the site for an additional 4 min. The wound was cleaned and closed. Each animal was injected with 6-OHDA on the right side only, producing hemi-Parkinsonian rats. After surgery, an analgesic (buprenorphine hydrochloride, 0.1 ml of 0.3 mg/ml) and an anti-inflammatory (meloxicam, 0.1 ml of 1.5 mg/ml) were subcutaneously injected.

MGE Transplant Surgery

Adult pregnant rats that expressed the green fluorescent protein (EGFP) under the chick-beta actin promoter (Wistar-TgN [CAG-GFP, 184Ys, Rat Resource and Research Center]) were anesthetized as described above. Fetuses were removed from the uterus at E14.5. Fetal brains and MGEs were dissected in oxygenated artificial cerebrospinal fluid (aCSF, in mm: NaCl, 125; KCl, 2.5; MgCl₂, 1; CaCl₂, 2; NaPO₄, 1.25; NaHCO₃, 25; and glucose, 25; Sigma). The MGE from both hemispheres of four animals was used to prepare dissociated cells for each surgery. The MGE tissue was mechanically dissociated in the presence of 1% DNase I in aCSF. Cells were centrifuged at 2× gravity for 2 min, and pellets were dissociated in 5 μl of aCSF. Immediately after dissociation, three injections were performed along the rostro-caudal axis of the striatum, and cells were deposited at three delivery sites along the dorsal-ventral axis at each injection site. 400 nl of cell suspension was injected at each delivery site for a total of 3.6 μl of MGE cell suspension injected each time. One 300 nl injection was performed into the subthalamic nucleus (STN). The total number of transplanted cells averaged 252,390 ± 7,729. Sham injections were performed as described above but only aCSF vehicle was injected. Dead MGE cells were obtained by freezing the MGE cell suspension at −20°C for 5 min, followed by 5 min at 37°C, and this cycle was repeated eight times (Modo et al., 2003).

Immunocytochemistry

Rats were anesthetized and perfused intracardially with 0.1 M phosphate buffer saline (PBS) followed by 4% paraformaldehyde in PBS at 4°C (PFA). The brains were removed and postfixed 24 hr in PFA. Coronal 50 μm slices were prepared on a vibratome (Leica). Free-floating sections were blocked

in 10% donkey serum (GIBCO, CA, USA), 0.1% Triton X-100 (Sigma, MO, USA), and 0.2% gelatin (Sigma). Sections were incubated 24 hr in primary antibodies at room temperature. The primary antibodies were: anti-neuronal specific nuclear protein (mouse anti-NeuN, 1:1000, Chemicon), gamma aminobutyric acid (rabbit anti-GABA, 1:1000, Sigma), glutamic acid decarboxylase 67 (mouse anti-GAD, 1:1000, Abcam), GABA transporter 1 (rabbit anti-GAT, 1:300, Abcam), CNPase (mouse anti-CNPase, 1:500, Abcam), glial fibrillary acidic protein (rabbit anti-GFAP, 1:1000, Sigma), substance P (rabbit anti-SP, 1:2000, Chemicon), somatostatin (mouse anti-Som, 1:100, Abcam), nitric oxide synthase (rabbit anti-NOS, 1:100, Abcam), choline acetyltransferase (rabbit anti-Chat, 1:500; Chemicon), tyrosine hydroxylase (mouse anti-TH, 1:1000, Boehringer Mannheim Biochemica), parvalbumin (mouse anti-PV, 1:1000, Chemicon), calretinin (mouse anti-CR, 1:1000; Chemicon), calbindin (mouse anti-CB, 1:2000; Swant, Bellinzona, Switzerland), synaptophysin (mouse anti-Synaptophysin, 1:200, Sigma), dopamine- and cAMP-regulated protein (rabbit anti-DARPP 32, 1:50, Abcam), dopamine transporter (rat anti-DAT, 1:500, Abcam), vesicular monoamine transporter 2 (rabbit anti-VMAT, 1:1000, Abcam), dopamine receptor 1 (rabbit anti-DR1, 1:2000, Abcam), dopamine receptor 2 (rabbit anti-DR2, 1:500, Abcam), and green fluorescent protein (chicken anti-GFP, 1:1000, Abcam). Sections were rinsed and incubated in the appropriate secondary antibody: Cy2, Cy3, or Cy5 conjugated polyclonal anti-mouse/goat/rabbit antibodies (1:100, Jackson Laboratories, ME, USA). Tissue was rinsed and mounted on coated glass slides and coverslipped with an aqueous mounting medium (Aquamount; Lerner, PA, USA). Confocal microscopy was performed on an Olympus Fluoview confocal laser scanning microscope and analysis performed in Fluoview v.3.3 (Olympus). We omitted the first antibody as a control for each immunostaining experiment.

Cell Quantification

The survival of MGE cells after transplantation and the percentage of transplanted MGE cells that expressed cell-specific markers were quantified through confocal microscopy. Brains were perfused and cut into 50 μm thick coronal sections. The number of MGE cells that survived transplantation was estimated by counting the number of cells in every third 50 μm thick section throughout the rostro-caudal axes of the brain and multiplying this number by three. The percentage of MGE-transplanted cells that expressed cell-type-specific markers was calculated with at least three animals for each marker (n = 27 total animals analyzed). MGE cells were counted in three coronal sections: one section at the level of a MGE cell transplantation, a second section 300 μm rostral to the injection, and a third section 300 μm caudal to the site of injection.

Electrophysiology

Coronal slices for electrophysiological recordings of GFP⁺ MGE-transplanted cells were prepared as described previously (Noctor et al., 2008). In brief, brains were sectioned at 400 μm with a vibratome (Leica) in ice-chilled aCSF containing (in mM) 25 glucose, 3 KCl, 1.25 NaH₂PO₄, 2 MgSO₄, 26 NaHCO₃, and 10 dextrose, saturated with 95% O₂/5% CO₂. Slices were incubated at 32°C for 30 min after slicing in NaCl-based ACSF containing (in mM) 126 NaCl, 3 KCl, 1.25 NaH₂PO₄, 2 MgSO₄, 26 NaHCO₃, 10 dextrose, and 2 CaCl₂, saturated with 95% O₂/5% CO₂. Slices were held at room temperature until being moved to a 32°C submersion-type chamber on an Olympus BX50WI upright microscope. GFP⁺ cells were identified under epifluorescence and recordings performed with either an EPC-9 patch-clamp amplifier (Heka Electronics) controlled by an Apple computer running Pulse v8.0 (Heka) or pClamp version 10 (Axon Instruments). Patch pipettes were made from 1.5 mm OD/1.0 mm ID glass (Corning) and filled with (in mM) 130 K-gluconate, 4 KCl, 2 NaCl, 10 HEPES, 0.2 EGTA, 4 ATP-Mg, 0.3 GTP-disodium, 14 phosphocreatine-dipotassium (pH 7.25, 280–290 mOsm). For morphological reconstruction, 50 μM Texas Red dextran (Molecular Probes) was included in the recording solution. For measurement of miniature synaptic currents, K-gluconate was replaced with KCl and osmolarity was adjusted with sucrose. GABAergic and glutamatergic minis were isolated in ACSF containing TTX (0.5 μM, Calbiochem) with bicuculline methiodide (100 μM, Sigma) and DNQX (20 μM, Tocris) with an Octaflow drug application system (ALA Scientific Instruments, Inc.). Series resistances were typically between 5 and 15 MΩ and were continually monitored and compensated for throughout the recording sessions. Voltages were corrected for a 14 mV liquid junction potential.

Recordings were performed with a MultiClamp 700B amplifier (Axon Instruments) under infrared-differential interference contrast visualization with an Olympus BX50WI and a CCD camera (MTI). Glass recording electrodes (7–10 MΩ) were filled with (in mM): KCl 130, NaCl 5, CaCl₂ 0.4, MgCl₂ 1, HEPES 10 [pH 7.3], EGTA 1.1, to which 500 μM Alexa 594-conjugated biocytin (Molecular Probes) was added to identify recorded cells. Recordings were acquired and analyzed with pClamp version 10 (Axon Instruments) and data were further analyzed in Excel (Microsoft, Inc.) and Mini Analysis (Synaptosoft). All averages reported appear as mean ± standard error. Resting membrane potential was measured immediately after breaking into whole-cell recording mode. Input resistance was calculated from small (3–5 mV) 600 ms voltage deflections induced by square hyperpolarizing current injections (averages of 20–40 deflections). Estimates of the membrane time constant were obtained by fitting an exponential function to these same hyperpolarizing voltage deflections. Input capacitance was calculated by dividing the time constant by the input resistance. Epifluorescent images of the recorded cells were collected with Scion Image and arranged with Photoshop.

Behavioral Tests

We performed behavioral tests at 3 and 5 weeks after the 6-OHDA surgeries; MGE cell, sham, and dead cell transplants were performed at week 6; and behavioral tests were repeated on weeks 9, 11, 14, and 18.

Rotational Behavior

Drug-induced rotations were measured in an automated rotometer bowl 28 cm in diameter × 36 cm high (Columbus Instruments, OH) (Ungerstedt and Arbuthnott, 1970). After intraperitoneal injection of apomorphine (0.05 mg/kg, i.p.), the animals were fitted with a jacket that was attached to a rotation sensor and placed in the test bowl. The number and direction of rotations was recorded over a test period of 40 min (Figure S1C). Apomorphine stimulates dopaminergic receptors directly, preferentially on the denervated side resulting from denervation-induced dopamine receptor supersensitivity, causing contralateral rotation (Creese et al., 1977; Ungerstedt, 1971; Ungerstedt and Arbuthnott, 1970). There is a threshold of SNc damage that must be reached in order to produce maximal rotation behavior after apomorphine administration (Hudson et al., 1993). The abnormal behavior of hemi-Parkinsonian rats is directly related to the amount of DA cell loss. We observed that less than 50% dopamine depletion in the striatum did not yield a significant change in rotation behavior after apomorphine injection, because of compensatory mechanisms in the striatum. For our experiment we selected only those 6-OHDA rats that rotated at least four times more to the contralateral than to the ipsilateral side of the injection.

Stride Test

The test animal was placed on a runway 1 m long and 33 cm wide with walls 50 cm high on either side. A dark enclosure was placed at one end of the runway, and rats were free to enter the enclosure after traversing the runway. Rats were trained to run down the runway by placing them on the runway at the end opposite to the dark enclosure. The floor of the runway was covered with paper. At the start of each test, the animals' rear feet were dipped in black ink before being placed at the beginning of the runway. We repeated the test twice for each rat, measured the length of stride for each test, and obtained an average stride length for each rat. We compared the average stride length across groups. 6-OHDA rats display impairments in the posture and movement of the contralateral limbs (Figures S1D and S1E).

Open Field Test

We used an Open Field 16 × 16 Photobeam System with Flex-Field software (40 cm wide, 40 cm deep, and 37.5 cm high, SD. Instruments). Each animal was placed in the center of the enclosure at the start of the test and allowed to freely explore the apparatus for 5 min. The Flex-Field software recorded units of movement, which were represented by the number of entries into each of the 256 square zones of the open field, and the amount of time spent at each point. At the end of the experiment, the movement of each rat during the 5 min period was represented as units of movement and by a zone map that traced the path followed by the rat in the open field.

Statistical Analysis

Data were analyzed with a 2-way ANOVA model with time and group (6-OHDA, 6-OHDA + MGE cells, 6-OHDA + sham surgery, and 6-OHDA + dead MGE cells) as factors. We ran a set of multiple comparisons for each dependent

variable (rotation, stride length, and width of path), based on the least-squares means (LSMeans), comparing groups averaged across time, or groups within each time point, expressed relative to the baseline observation. The results were expressed in terms of dependent variable (the response measure), the time point being analyzed relative to the baseline value, the p value for overall ANOVA, and the multiple comparisons. Because of the existence of occasional outliers (extreme observations), the rotation data did not satisfy the ANOVA assumption that the residual errors were normally distributed. To address this issue, the rotation data (the number of turns in the contralateral direction) was log-transformed. We ran behavioral tests on two time points before MGE treatment (weeks 3 and 5) and on four time points after MGE treatment (weeks 9, 11, 14, and 18). We used the week 5 observation time point as the baseline point and expressed the results of each subsequent behavioral test relative to the week 5 results. We performed a series of multiple observations among the four groups (6-OHDA, 6-OHDA + MGE cells, 6-OHDA + sham surgery, and 6-OHDA + dead MGE cells). Graphs display the change from base line measures.

SUPPLEMENTAL INFORMATION

Supplemental Information includes Supplemental Experimental Procedures and one figure and can be found with this article online at doi:10.1016/j.stem.2010.01.004.

REFERENCES

Alvarez-Dolado, M., Calcagnotto, M.E., Karkar, K.M., Southwell, D.G., Jones-Davis, D.M., Estrada, R.C., Rubenstein, J.L., Alvarez-Buylla, A., and Baraban, S.C. (2006). Cortical inhibition modified by embryonic neural precursors grafted into the postnatal brain. J. Neurosci. 26, 7380–7389.

Anderson, S.A., Eisenstat, D.D., Shi, L., and Rubenstein, J.L. (1997a). Interneuron migration from basal forebrain to neocortex: Dependence on Dlx genes. Science 278, 474–476.

Anderson, S.A., Qiu, M., Bulfone, A., Eisenstat, D.D., Meneses, J., Pedersen, R., and Rubenstein, J.L. (1997b). Mutations of the homeobox genes Dlx-1 and Dlx-2 disrupt the striatal subventricular zone and differentiation of late born striatal neurons. Neuron 19, 27–37.

Anderson, S., Mione, M., Yun, K., and Rubenstein, J.L. (1999). Differential origins of neocortical projection and local circuit neurons: Role of Dlx genes in neocortical interneuronogenesis. Cereb. Cortex 9, 646–654.

Benabid, A.L., Koudsié, A., Benazzouz, A., Fraix, V., Ashraf, A., Le Bas, J.F., Chabardes, S., and Pollak, P. (2000). Subthalamic stimulation for Parkinson's disease. Arch. Med. Res. 31, 282–289.

Berger, K., Przedborski, S., and Cadet, J.L. (1991). Retrograde degeneration of nigrostriatal neurons induced by intrastriatal 6-hydroxydopamine injection in rats. Brain Res. Bull. 26, 301–307.

Butt, S.J., Fuccillo, M., Nery, S., Noctor, S., Kriegstein, A., Corbin, J.G., and Fishell, G. (2005). The temporal and spatial origins of cortical interneurons predict their physiological subtype. Neuron 48, 591–604.

Campbell, K., Olsson, M., and Björklund, A. (1995). Regional incorporation and site-specific differentiation of striatal precursors transplanted to the embryonic forebrain ventricle. Neuron 15, 1259–1273.

Creese, I., Burt, D.R., and Snyder, S.H. (1977). Dopamine receptor binding enhancement accompanies lesion-induced behavioral supersensitivity. Science 197, 596–598.

Daadi, M.M., Lee, S.H., Arac, A., Grueter, B.A., Bhatnagar, R., Maag, A.L., Schaar, B., Malenka, R.C., Palmer, T.D., and Steinberg, G.K. (2009). Functional engraftment of the medial ganglionic eminence cells in experimental stroke model. Cell Transplant. 18, 815–826.

Dahl, C.B., and Götestam, K.G. (1989). An open field study of antidepressant drugs. Pharmacol. Toxicol. 64, 302–307.

Deacon, T.W., Pakzaban, P., and Isacson, O. (1994). The lateral ganglionic eminence is the origin of cells committed to striatal phenotypes: Neural transplantation and developmental evidence. Brain Res. 668, 211–219.

Defelipe, J., González-Albo, M.C., Del Río, M.R., and Elston, G.N. (1999). Distribution and patterns of connectivity of interneurons containing calbindin, calretinin, and parvalbumin in visual areas of the occipital and temporal lobes of the macaque monkey. J. Comp. Neurol. 412, 515–526.

DeLong, M.R., and Wichmann, T. (2007). Circuits and circuit disorders of the basal ganglia. Arch. Neurol. 64, 20–24.

Du, Y., and Dreyfus, C.F. (2002). Oligodendrocytes as providers of growth factors. J. Neurosci. Res. 68, 647–654.

During, M.J., Kaplitt, M.G., Stern, M.B., and Eidelberg, D. (2001). Subthalamic GAD gene transfer in Parkinson disease patients who are candidates for deep brain stimulation. Hum. Gene Ther. 12, 1589–1591.

Goto, S., Yamada, K., Yoshikawa, M., Okamura, A., and Ushio, Y. (1997). GABA receptor agonist promotes reformation of the striatonigral pathway by transplant derived from fetal striatal primordia in the lesioned striatum. Exp. Neurol. 147, 503–509.

Grasbon-Frodl, E.M., Nakao, N., Lindvall, O., and Brundin, P. (1997). Developmental features of human striatal tissue transplanted in a rat model of Huntington's disease. Neurobiol. Dis. 3, 299–311.

Hudson, J.L., van Horne, C.G., Strömberg, I., Brock, S., Clayton, J., Masserano, J., Hoffer, B.J., and Gerhardt, G.A. (1993). Correlation of apomorphine- and amphetamine-induced turning with nigrostriatal dopamine content in unilateral 6-hydroxydopamine lesioned rats. Brain Res. 626, 167–174.

Kaplitt, M.G., Feigin, A., Tang, C., Fitzsimons, H.L., Mattis, P., Lawlor, P.A., Bland, R.J., Young, D., Strybing, K., Eidelberg, D., and During, M.J. (2007). Safety and tolerability of gene therapy with an adeno-associated virus (AAV) borne GAD gene for Parkinson's disease: an open label, phase I trial. Lancet 369, 2097–2105.

Kawaguchi, Y. (1993). Physiological, morphological, and histochemical characterization of three classes of interneurons in rat neostriatum. J. Neurosci. 13, 4908–4923.

Kawaguchi, Y. (1997). Neostriatal cell subtypes and their functional roles. Neurosci. Res. 27, 1–8.

Kawaguchi, Y., Wilson, C.J., Augood, S.J., and Emson, P.C. (1995). Striatal interneurones: Chemical, physiological and morphological characterization. Trends Neurosci. 18, 527–535.

Koós, T., and Tepper, J.M. (1999). Inhibitory control of neostriatal projection neurons by GABAergic interneurons. Nat. Neurosci. 2, 467–472.

Koos, T., Tepper, J.M., and Wilson, C.J. (2004). Comparison of IPSCs evoked by spiny and fast-spiking neurons in the neostriatum. J. Neurosci. 24, 7916–7922.

Kubota, Y., Hattori, R., and Yui, Y. (1994). Three distinct subpopulations of GABAergic neurons in rat frontal agranular cortex. Brain Res. 649, 159–173.

Larsson, E., Lindvall, O., and Kokaia, Z. (2001). Stereological assessment of vulnerability of immunocytochemically identified striatal and hippocampal neurons after global cerebral ischemia in rats. Brain Res. 913, 117–132.

Lavdas, A.A., Grigoriou, M., Pachnis, V., and Parnavelas, J.G. (1999). The medial ganglionic eminence gives rise to a population of early neurons in the developing cerebral cortex. J. Neurosci. 19, 7881–7888.

Lee, B., Lee, H., Nam, Y.R., Oh, J.H., Cho, Y.H., and Chang, J.W. (2005). Enhanced expression of glutamate decarboxylase 65 improves symptoms of rat parkinsonian models. Gene Ther. *12*, 1215–1222.

Litvan, I., Halliday, G., Hallett, M., Goetz, C.G., Rocca, W., Duyckaerts, C., Ben-Shlomo, Y., Dickson, D.W., Lang, A.E., Chesselet, M.F., et al. (2007). The etiopathogenesis of Parkinson disease and suggestions for future research. Part I. J. Neuropathol. Exp. Neurol. *66*, 251–257.

Ljungberg, T., and Ungerstedt, U. (1976). Automatic registration of behaviour related to dopamine and noradrenaline transmission. Eur. J. Pharmacol. *36*, 181–188.

Luk, K.C., and Sadikot, A.F. (2001). GABA promotes survival but not proliferation of parvalbumin-immunoreactive interneurons in rodent neostriatum: An in vivo study with stereology. Neuroscience *104*, 93–103.

Luo, J., Kaplitt, M.G., Fitzsimons, H.L., Zuzga, D.S., Liu, Y., Oshinsky, M.L., and During, M.J. (2002). Subthalamic GAD gene therapy in a Parkinson's disease rat model. Science *298*, 425–429.

Mallet, N., Ballion, B., Le Moine, C., and Gonon, F. (2006). Cortical inputs and GABA interneurons imbalance projection neurons in the striatum of parkinsonian rats. J. Neurosci. *26*, 3875–3884.

Marin, O., Anderson, S.A., and Rubenstein, J.L. (2000). Origin and molecular specification of striatal interneurons. J. Neurosci. *20*, 6063–6076.

Modo, M., Stroemer, R.P., Tang, E., Patel, S., and Hodges, H. (2003). Effects of implantation site of dead stem cells in rats with stroke damage. Neuroreport *14*, 39–42.

Noctor, S.C., Martinez-Cerdeno, V., and Kriegstein, A.R. (2008). Distinct behaviors of neural stem and progenitor cells underlie cortical neurogenesis. J. Comp. Neurol. *508*, 28–44.

Olsson, M., Campbell, K., Wictorin, K., and Björklund, A. (1995). Projection neurons in fetal striatal transplants are predominantly derived from the lateral ganglionic eminence. Neuroscience *69*, 1169–1182.

Olsson, M., Bentlage, C., Wictorin, K., Campbell, K., and Björklund, A. (1997). Extensive migration and target innervation by striatal precursors after grafting into the neonatal striatum. Neuroscience *79*, 57–78.

Olsson, M., Björklund, A., and Campbell, K. (1998). Early specification of striatal projection neurons and interneuronal subtypes in the lateral and medial ganglionic eminence. Neuroscience *84*, 867–876.

Paxinos, G., and Watson, C. (1982). The Rat Brain in Stereotaxic Coordinates (New York: Academic Press).

Piccini, P. (2002). Dyskinesias after transplantation in Parkinson's disease. Lancet Neurol. *1*, 472.

Plenz, D., and Kitai, S.T. (1998). Up and down states in striatal medium spiny neurons simultaneously recorded with spontaneous activity in fast-spiking interneurons studied in cortex-striatum-substantia nigra organotypic cultures. J. Neurosci. *18*, 266–283.

Pow, D.V., Sullivan, R.K., Williams, S.M., Scott, H.L., Dodd, P.R., and Finkelstein, D. (2005). Differential expression of the GABA transporters GAT-1 and GAT-3 in brains of rats, cats, monkeys and humans. Cell Tissue Res. *320*, 379–392.

Rymar, V.V., Sasseville, R., Luk, K.C., and Sadikot, A.F. (2004). Neurogenesis and stereological morphometry of calretinin-immunoreactive GABAergic interneurons of the neostriatum. J. Comp. Neurol. *469*, 325–339.

Salin, P., López, I.P., Kachidian, P., Barroso-Chinea, P., Rico, A.J., Gómez-Bautista, V., Coulon, P., Kerkerian-Le Goff, L., and Lanciego, J.L. (2009). Changes to interneuron-driven striatal microcircuits in a rat model of Parkinson's disease. Neurobiol. Dis. *34*, 545–552.

Tepper, J.M., and Bolam, J.P. (2004). Functional diversity and specificity of neostriatal interneurons. Curr. Opin. Neurobiol. *14*, 685–692.

Terpstra, B.T., Collier, T.J., Marchionini, D.M., Levine, N.D., Paumier, K.L., and Sortwell, C.E. (2007). Increased cell suspension concentration augments the survival rate of grafted tyrosine hydroxylase immunoreactive neurons. J. Neurosci. Methods *166*, 13–19.

Ungerstedt, U. (1971). Striatal dopamine release after amphetamine or nerve degeneration revealed by rotational behaviour. Acta Physiol. Scand. Suppl. *367*, 49–68.

Ungerstedt, U., and Arbuthnott, G.W. (1970). Quantitative recording of rotational behavior in rats after 6-hydroxy-dopamine lesions of the nigrostriatal dopamine system. Brain Res. *24*, 485–493.

West, M.J., Ostergaard, K., Andreassen, O.A., and Finsen, B. (1996). Estimation of the number of somatostatin neurons in the striatum: An in situ hybridization study using the optical fractionator method. J. Comp. Neurol. *370*, 11–22.

Wichterle, H., Garcia-Verdugo, J.M., Herrera, D.G., and Alvarez-Buylla, A. (1999). Young neurons from medial ganglionic eminence disperse in adult and embryonic brain. Nat. Neurosci. *2*, 461–466.

Wilkins, A., Majed, H., Layfield, R., Compston, A., and Chandran, S. (2003). Oligodendrocytes promote neuronal survival and axonal length by distinct intracellular mechanisms: A novel role for oligodendrocyte-derived glial cell line-derived neurotrophic factor. J. Neurosci. *23*, 4967–4974.

Winkler, C., Bentlage, C., Nikkhah, G., Samii, M., and Björklund, A. (1999). Intranigral transplants of GABA-rich striatal tissue induce behavioral recovery in the rat Parkinson model and promote the effects obtained by intrastriatal dopaminergic transplants. Exp. Neurol. *155*, 165–186.

Zhao, Y., Marín, O., Hermesz, E., Powell, A., Flames, N., Palkovits, M., Rubenstein, J.L., and Westphal, H. (2003). The LIM-homeobox gene Lhx8 is required for the development of many cholinergic neurons in the mouse forebrain. Proc. Natl. Acad. Sci. USA *100*, 9005–9010.